Journal of Visualized Experiments

Time-Lapse Imaging of Mouse Macrophage Chemotaxis

--Manuscript Draft--

Article Type:	Invited Methods Article - JoVE Produced Video
Manuscript Number:	JoVE60750R1
Full Title:	Time-Lapse Imaging of Mouse Macrophage Chemotaxis
Section/Category:	JoVE Immunology and Infection
Keywords:	Mouse; macrophages; motility; chemotaxis; live-cell imaging; time-lapse imaging; complement receptor C5a
Corresponding Author:	Peter J. Hanley Institut fuer Molekulare Zellbiologie Muenster, GERMANY
Corresponding Author's Institution:	Institut fuer Molekulare Zellbiologie
Corresponding Author E-Mail:	hanley@uni-muenster.de
Order of Authors:	Peter J. Hanley
	Esther van den Bos
	Stefan Walbaum
	Markus Horsthemke
	Anne C. Bachg
Additional Information:	
Question	**Response**
Please indicate whether this article will be Standard Access or Open Access.	Open Access (US$4,200)
Please indicate the **city, state/province, and country** where this article will be **filmed**. Please do not use abbreviations.	Muenster, Nordrhein-Westfalen, Germany

TITLE:

Time-Lapse Imaging of Mouse Macrophage Chemotaxis

AUTHORS AND AFFILIATIONS:

Esther van den Bos[1], Stefan Walbaum[1], Markus Horsthemke[1], Anne C. Bachg[1], Peter J. Hanley[1]

[1]Institut für Molekulare Zellbiologie, Münster, Germany

Corresponding Author:

Peter J. Hanley (hanley@uni-muenster.de)

Email Addresses of Co-Authors:

Esther van den Bos (e_vand08@uni-muenster.de)
Stefan Walbaum (stefan.walbaum@uni-muenster.de)
Markus Horsthemke (marhorst@uni-muenster.de)
Anne C. Bachg (a_bach08@uni-muenster.de)

KEYWORDS:

mouse, macrophages, motility, chemotaxis, live-cell imaging, time-lapse imaging, complement receptor C5a

SUMMARY:

Here we describe methods using time-lapse, phase-contrast microscopy to image mouse resident peritoneal macrophages in a chemotactic complement C5a gradient. The protocols can be extended to other immune cells.

ABSTRACT:

Chemotaxis is receptor-mediated guidance of cells along a chemical gradient, whereas chemokinesis is the stimulation of random cell motility by a chemical. Chemokinesis and chemotaxis are fundamental for the mobilization and deployment of immune cells. For example, chemokines (chemotactic cytokines) can rapidly recruit circulating neutrophils and monocytes to extravascular sites of inflammation. Chemoattractant receptors belong to the large family of G protein-coupled receptors. How chemoattractant (i.e., ligand) gradients direct cell migration via G protein-coupled receptor signaling is not yet fully understood. In the field of immunology, neutrophils are popular model cells for studying chemotaxis in vitro. Here we describe a real-time two-dimensional (2D) chemotaxis assay tailored for mouse resident macrophages, which have traditionally been more difficult to study. Macrophages move at a slow pace of ~1 µm/min on a 2D surface and are less well suited for point-source migration assays (e.g., migration towards the tip of a micropipette filled with chemoattractant) than neutrophils or *Dictyostelium discoideum*, which move an order of magnitude faster. Widely used Transwell assays are useful for studying the chemotactic activity of different substances, but do not provide information on cell morphology, velocity, or chemotactic navigation. Here we describe a time-lapse microscopy-based macrophage chemotaxis assay that allows quantification of cell velocity and chemotactic efficiency and provides a platform to delineate the transducers, signal pathways, and effectors

of chemotaxis.

INTRODUCTION:

Immune cells typically migrate singly on a 2D surface in an amoeboid fashion[1,2], which involves repeated cycles of protrusion of the front, integrin-mediated cell adhesion, and retraction of the rear. A prerequisite step is cell polarization, in which cells form front and rear ends[3]. Chemotaxis starts with the detection of chemoattractants by G protein-coupled receptors and a complex signaling network mediated by membrane-anchored heterotrimeric G proteins and small monomeric G proteins, as well as phospholipid-bound guanine nucleotide exchange factors (GEFs)[4,5]. Activation of Rho GTPases of the Cdc42 and Rac subfamilies induce protrusions at the front[6] and members of the Rho subfamily, especially RhoA, activate contraction of the rear[5,7]. In a three-dimensional (3D) environment, integrins are largely redundant for leukocyte migration and RhoA becomes more important for squeezing cells through narrow passages[8], whereas Cdc42- or Rac-induced Arp2/3 activation remains important for chemotactic steering[9,10].

Immune cells may face different chemoattractants, especially in the settings of tissue injury, pathogen invasion, and inflammation. The endogenous chemoattractants expressed on phagocytes complement C3a and C5a, are rapidly generated by activation of the complement cascade, and are recognized by complement C3a and C5a receptors. Similarly, necrotic cells recruit phagocytes via formyl peptide receptors, which recognize mitochondria-derived as well as bacteria-derived formyl peptides[11]. Immune cells also express G protein-coupled receptors for chemokines, a large family of chemoattractant peptides involved in the regulation of immune cell trafficking during both homeostasis and inflammation. Chemokines are classified into four groups depending on the spacing of the first two cysteine (C) residues: C, CC, CXC, and CX_3C cytokines, where X is an amino acid. Thus, in vivo immune cells need to appropriately respond to highly complex spatial and temporal signals, making the study of chemotaxis a daunting task. Below we provide a brief history of chemotaxis, which began with intravital imaging approaches.

The study of leukocyte chemotaxis dates back to 1888[12], when the ophthalmologist Theodor Karl Gustav Leber clearly described the directed migration of leukocytes to, and the accumulation at, sites of inflammation in a model of mycotic (fungal) keratitis. Leber stressed that the attraction of excess leukocytes by pathogen-derived substances is important for elimination of harmful microorganisms via phagocytosis, which had been described by Metchnikoff (also known as Metschnikoff) earlier in the same decade[13]. In vivo experiments were also performed in the 1920s by Clark and Clark[14,15], who took advantage of the transparency of tadpoles and showed that sterile inflammation induced by croton oil[14] or other irritants[15] caused leukocytes to adhere to blood vessels, followed by diapedesis (transendothelial migration) and rapid migration through the tissue spaces towards the irritant. In vitro experiments using the microcinematography method developed by Jean Comandon[16] showed that leukocytes migrated towards a particulate chemoattractant source such as bacteria[17]. At that time, the molecular identities of chemotactic factors were unknown. In the 1960s, Stephen Boyden[18] recognized that techniques to study the chemotactic activity of soluble substances were lacking. He devised a chamber, subsequently known as the Boyden chamber, with two compartments separated by a filter paper membrane. A cell suspension is added to the upper compartment and the test substance is added to either

both compartments or only to the lower compartment. After an incubation period, the filter membrane is removed, and the cells are fixed and stained. By comparing how many cells migrate across the filter membrane towards the lower well with the test substance in both compartments, in neither compartment, or only in the lower compartment, chemotactic activity can be determined. Transwell assays are still popular today and have been modified in various ways, including the use of different polycarbonate membranes with defined pore sizes and densities[19,20]. A major drawback of Transwell assays is that it is impractical to directly visualize cells migrating and the migration path across the membrane typically does not exceed the diameter of an immune cell.

Sally H. Zigmond developed a chemotaxis chamber[21] that enabled visualization of both gradient formation and cell morphology using fluorescent dyes. The chamber consists of a plexiglass (acrylic) slide with two parallel linear wells, each with a volume of ~100 µL, separated by a 1 mm wide bridge 3–10 µm below the upper plane of the slide. A coverslip seeded with cells is inverted and placed onto the slide such that it spans the two wells. After addition of a chemoattractant to one of the wells, a steep chemoattractant gradient forms across the bridge, typically within 30–90 min. Human polymorphonuclear leukocytes (granulocytes) in the Zigmond chamber are observed orienting themselves towards the chemoattractant. Variations of the Zigmond chamber have been reported, including the Dunn[22] and Insall[23] chambers, both of which use a coverslip seeded with cells placed across two wells separated by a 1 mm wide bridge. The Dunn chamber consists of concentric wells separated by a circular bridge, whereas the Insall chamber is more closely related to the Zigmond chamber, but provides bridges of two different widths, 0.5 mm and 1 mm. A novel chemotaxis chamber, termed µ-Slide Chemotaxis and manufactured by plastic injection molding, was described by Zemgel et al.[24]. The chemotaxis chamber consists of two 40 µL reservoirs separated by a 1 mm wide channel with a length of 2 mm and a height of 70 µm. The bottom of the chamber is formed by a gas permeable, thin plastic sheet with the same thickness and optical properties of a No. 1.5 glass coverslip[24]. Here we describe a chemotaxis assay using the µ-Slide Chemotaxis chamber to visualize the migration of mouse resident peritoneal macrophages for up to 14 h in a chemotactic (complement C5a) gradient.

PROTOCOL:

The protocols follow the guidelines of our local research ethics committee, as well as the animal care guidelines.

NOTE: **Figure 1** shows a workflow of the chemotaxis assay.

1. Prefilling chemotaxis slides

1.1. Prefill the 1 mm wide and 2 mm long connecting channels of one or two chemotaxis slides using modified RPMI 1640 HEPES medium, consisting of bicarbonate-free RPMI 1640 medium containing 20 mM 4-(2-hydroxyethyl)-1-piperazineethanesulfonic acid (HEPES), 10% heat-inactivated fetal bovine serum (FBS), and antibiotics such as penicillin (100 units/mL) and streptomycin (100 µg/mL), prepared by diluting 100x penicillin/streptomycin, and 1 µg/mL

lipopolysaccharide (from *E. coli*), and a Toll-like receptor 4 ligand used to activate the cells.

1.1.1. Place a chemotaxis slide (**Figure 2A**) into a round (10 cm diameter) cell culture dish, both preheated to 37 °C, and set the dish onto a heated (37 °C) aluminum block. Insert plugs into ports 1 and 4 (**Figure 2B**).

NOTE: An aluminum block maintained at 37 °C and placed inside the laminar flow hood is useful for preparing chemotaxis chambers. Ideally, the heated block should provide a flat working area and wells for various tubes, such as 50 mL tubes and 2 mL microcentrifuge tubes.

1.1.2. Using a 10–200 µL pipette tip with a beveled tip, deposit 15 µL of modified RPMI 1640 HEPES medium into filling port 3 (**Figure 2B**). Next, with the volume still set at 15 µL and the control button of the (2–20 µL volume) pipette depressed, insert the pipette tip into port 2 and aspirate 15 µL at a moderately fast rate (**Figure 2B**). This will prefill the 1 mm x 2 mm connecting channel (observation area), as well as the two flanking supply channels (between the central observation area and ports 2 and 3, respectively). Cover filling ports 2 and 3 with caps.

1.1.3. After prefilling, place the chemotaxis slides onto a rack kept in a closed humidity chamber within an otherwise dry and CO_2-free incubator at 37 °C.

NOTE: It is important to use the correct pipette tip for filling the chemotaxis slide. A beveled pipette tip wedges into the top of the filling port, whereas commonly used pointed pipette tips can be inserted more deeply into the filling port and may greatly increase resistance to fluid flow.

2. Isolation of mouse resident peritoneal macrophages

2.1. Sacrifice a 3–4 month-old mouse using a high concentration of the volatile anesthetic isoflurane (>5% in air) or carbon dioxide[25], followed by cervical dislocation. Loss of the righting reflex in rodents correlates with loss of consciousness in humans[26]. Clean the abdomen of the mouse with 80% ethanol in water and then make a 1–2 cm midline skin incision using surgical scissors with blunt tips. Peel back the skin to expose the underlying abdominal wall.

2.2. Insert a 24 G plastic catheter into the peritoneal cavity. Using a 5 mL plastic syringe, lavage the cavity using 2 x 4.5 mL ice-cold Hank's buffered salt solution (HBSS), without Ca^{2+} and Mg^{2+}. Leave around 0.5 mL of residual HBSS in the syringe so that tissue inadvertently sucked onto the tip of the catheter can be expelled.

2.3. Transfer the lavaged medium, typically 8–8.5 mL in total, into a 14 mL polypropylene round bottom tube. Centrifuge the tube at 300 x *g* for 6.5 min at room temperature.

NOTE: The round bottom tube allows the supernatant to be fully decanted and reduces cell clumping.

2.4. Discard the supernatant and resuspend the peritoneal cells (typically ~4 x 10^6 cells per

mouse) in 200 µL of modified RPMI 1640 HEPES medium. Dilute a sample of the cell suspension 1:20 and use a counting device, such as a Neubauer improved counting chamber, to count the cells. Next, dilute the cell suspension to a final concentration of 10 x 10^6 cells/mL and maintain the cells in a round bottom 2 mL polypropylene microcentrifuge tube at 37 °C using a heated aluminum block (see NOTE in step 1.1.1).

3. Seeding peritoneal cells into chemotaxis slides

3.1. After pipetting the cell suspension up and down 5x with the pipette volume set at 100 µL (or at half the suspension volume) to reduce clumping, gently deposit 10 µL of the cell suspension into port 3 of a chemotaxis chamber (**Figure 2C**). Place the pipette tip into port 2 and slowly draw the cell suspension into the connecting channel (**Figure 2C**). As soon as the cell suspension has been introduced, remove the plugs at ports 1 and 4, which will help to arrest the flow of the cell suspension. Place caps on all four filling ports.

3.2. Repeat step 3.1 for all chemotaxis chambers. Using a small inverted microscope and a 10x phase-contrast objective lens, inspect the chemotaxis slides for unwanted air bubbles.

3.3. Place the chemotaxis slides seeded with peritoneal cells in a humidity chamber at 37 °C for 2–3 h.

4. Filling the reservoirs and adding chemoattractant

4.1. Inspect the observation area (channel connecting the two 40 µL reservoirs) using an inverted microscope.

NOTE: At this stage, the cell density will be higher than after filling the reservoirs, because weakly adherent cells, predominantly $CD19^+$ cells (B1 cells), will be washed out of the observation area during the filling procedure (**Figure 2C–E**).

4.2. Place plugs into filling ports 1 and 2 (**Figure 2D**). Ensure that filling port 3 is filled to the top with medium and free of air bubbles. Use a sterile 27 G syringe needle to dislodge unwanted air bubbles, if required.

4.3. Using a 10–100 µL volume mechanical pipette, aspirate ~60 µL of modified RPMI 1640 HEPES medium and place the pipette tip into filling port 3. Use the volume setting ring of the pipette to slowly and steadily inject medium into the reservoir such that medium reaches the top of filling port 4 after 1–2 min (**Figure 2D**).

4.4. Fill the second reservoir. Move the plug from port 1 and slowly insert it into port 3 (**Figure 2D**). Next, aspirate ~50 µL of modified RPMI 1640 HEPES medium and place the pipette tip into filling port 4. Use the volume setting ring of the 10–100 µL volume pipette to slowly and steadily inject medium into the second reservoir such that medium reaches the top of filling port 1 after 1–2 min (**Figure 2D**).

4.5. Place 495 µL of modified RPMI 1640 HEPES medium into a (round bottom) 2 mL microcentrifuge tube and add 5 µL of Patent Blue V (stock solution: 10 mg/mL in phosphate-buffered saline [PBS]), a blue dye used as a visual indicator of concentration gradient formation. Mix by brief vortexing. Add 5.4 µL of recombinant mouse complement C5a (stock solution: 50 µg/mL in PBS with 0.1% bovine serum albumin) and mix by brief vortexing.

4.6. Deposit 15 µL of blue, complement C5a-containing medium into filling port 1 (**Figure 3A**), after making sure that the shallow depression at the top of the port is medium free (otherwise the drop may spillover).

4.7. Insert a 10–200 µL pipette tip into filling port 4 and slowly and steadily rotate the volume setting ring of the 10–100 µL volume pipette to draw the drop of blue, complement C5a-containing medium into the opposite reservoir (**Figure 3B**). Air will start to enter the short vertical column of filling port 1. Draw air in until the fluid-air interface is midway in the vertical column, and then slowly insert a plug into the port.

4.8. Gently lift the pipette from port 4, using the other hand to ensure that the slide remains fixed in place. Finally, slowly plug port 4 (**Figure 3B**).

4.9. Inspect the chemotaxis slide on an inverted microscope.

NOTE: The remaining adherent cells in the observation area should be predominantly macrophages. This can be confirmed using fluorescently tagged anti-F4/80 antibodies (F4/80 is a specific marker for mouse macrophages). B cells can be identified using fluorescently tagged anti-CD19 antibodies and $F4/80^{-}/CD19^{-}$ cells can be detected using a blue fluorescent nucleic acid stain (**Figure 4**).

5. Imaging macrophage migration by time-lapse, phase-contrast microscopy

5.1. Place a chemotaxis slide on the stage of an inverted microscope fitted with a stage incubator. Maintain the temperature at 37 °C.

5.2. Image the 1 mm x 2 mm observation area using a 10x phase-contrast objective lens and focus on the macrophage lamellipodia: thin, sheet-like membrane protrusions. Capture images for 14 h at a rate of 1 frame every 2 min.

6. Analysis of time-lapse images

6.1. Analyze the time-lapse, phase-contrast images using automated image analysis software or the Manual Tracking plugin, produced by Fabrice P. Cordelières, for ImageJ.

NOTE: Automated tracking programs can be used to analyze cells imaged by either time-lapse, phase-contrast, or fluorescence microscopy. For example, the Java-based software iTrack4U

produced by Cordelières et al.[27] can be used for automated cell tracking and analysis using time-lapse, phase-contrast, or fluorescence images as input. Manual tracking is more time consuming, but the tracks generated by the ImageJ plugin Manual Tracking can be directly imported and automatically analyzed by the ImageJ plugin Chemotaxis and Migration Tool[28,29].

REPRESENTATIVE RESULTS:

A schematic diagram of the chemotaxis slide used for time-lapse video microscopy of mouse peritoneal macrophages migrating in a chemotactic gradient is shown in **Figure 2A**. The slide contains three chemotaxis chambers, each of which has four filling ports. Ports can be individually closed using the plugs shown above the slide. Alternatively, a non-sealing cap can be placed over an unplugged port to maintain sterility. After plugging ports 1 and 4, the observation area (1 mm wide x 2 mm long x 70 µm high channel connecting the two reservoirs) between ports 2 and 3 can be prefilled with medium by placing a 15 µL drop into port 3 and aspirating with a 2–20 µL volume pipette at port 2 (**Figure 2B**). A suspension of mouse resident peritoneal cells (10 x 10^6 cells/mL) was seeded into the observation area by placing a 10 µL drop of suspension into port 3 and slowly aspirating at port 2 (**Figure 2C**). A typical image of cells seeded in the observation area taken by phase-contrast microscopy using a 10x objective lens is shown in **Figure 2C**. After incubating for 2–3 h, the chemotaxis slide was slowly filled with medium (**Figure 2D**). After plugging ports 1 and 2, medium was slowly injected via port 3 until it emerged from port 4. Next, the plug was switched from port 1 to port 3, and then the second reservoir was filled by slowly injecting medium via port 4 until it emerged at port 1. At this stage, cells in the observation area were reinspected using an inverted microscope (**Figure 2E**). By comparing images shortly before (**Figure 2C**) and after (**Figure 2E**) filling of the reservoirs, up to two-thirds of the cells had been washed out of the observation area. Generally, weakly adherent $CD19^+$ cells (B1 cells) were washed out and the remaining cells were predominantly $F4/80^+$ cells (macrophages). This was demonstrated by fluorescence microscopy after labeling each cell type with fluorescently labeled specific antibodies (**Figure 4**). In **Figure 4A**, freshly isolated mouse resident peritoneal cells were labeled with green fluorescent fluorophore-conjugated anti-F4/80 antibodies and red fluorescent fluorophore-conjugated anti-CD19 antibodies, and the nuclei of cells were labeled with a blue fluorescent nucleic acid stain. F4/80 is a specific marker for mouse macrophages[30], whereas CD19 is a B cell marker. **Figure 4B** shows $F4/80^+$ cells imaged by spinning disk confocal microscopy in the observation area of a chemotaxis chamber. The cells were labeled after an overnight chemotaxis assay recorded by time-lapse, phase-contrast microscopy.

Complement C5a (chemoattractant) was introduced to one of the two reservoirs by placing a 15 µL drop of medium containing 0.54 µg/mL (recombinant mouse) complement C5a and 10 µg/mL Patent Blue V into filling port 1 (**Figure 3A**) after plugging ports 2 and 3. The chemoattractant medium was slowly drawn into the reservoir by slow aspiration with a pipette via port 4. **Figure 3B** shows the diffusion of the blue dye after drawing the 15 µL drop into a reservoir. Patent Blue V was used as an indirect visual indicator of chemoattractant diffusion. Complement C5a molecules are considerably larger than those of Patent Blue V (9.0 kDa versus 0.57 kDa) and diffuse more slowly. After diffusion of complement C5a in the reservoir, its concentration was ~0.2 µg/mL (15 µL/40 µL [reservoir volume] x 0.54 µg/mL = 0.2 µg/mL), equivalent to ~22.5 nM. A modestly steep gradient formed across the observation area after 3 h and continued to

increase, reaching a maximum at around 12 h[31]. **Figure 3C** shows the migration tracks of macrophages migrating in a complement C5a gradient, between 6–12 h after adding the chemoattractant. Cell velocity and chemotactic efficiency, indexed as y-FMI (y-forward migration index; range: -1–+1) and x-FMI, of individual macrophages was calculated from the migration plots (**Figure 3D**). **Figure 3D** also shows a migration plot produced after normalizing the start point of each migration track to X = 0 and Y = 0 below the box plots. The inset in the migration plot shows how the y-FMI was calculated for each migration track.

FIGURE LEGENDS:

Figure 1: The workflow of the chemotaxis assay.

Figure 2: Handling of chemotaxis slides. (**A**) A 3D view of a chemotaxis slide with four plugs and four caps. The slide contains three chemotaxis chambers, each of which consists of two 40 µL reservoirs connected by a 1 mm x 2 mm channel, which is 70 µm high, termed the observation area. (**B**) The connecting channel extends at both ends to filling ports 2 and 3. After inserting plugs into filling ports 1 and 4, the observation area was prefilled with medium (red) by applying a drop of medium to port 3 and aspirating at port 2 with a 10–200 µL pipette tip. Subsequently, caps were applied to ports 2 and 3 before incubating the slide at 37 °C and preparing the cell suspension. (**C**) The observation area, where the chemoattractant gradient formed, was seeded with macrophages by applying a 10 µL drop of mouse resident peritoneal cells at port 3 and slowly aspirating at port 2. The slide was then incubated in a humidity chamber at 37 °C for 2–3 h. The phase-contrast image shown on the right, obtained via a 10x objective lens, shows peritoneal cells after seeding and incubation at 37 °C for 2 h. Scale bar = 500 µm. (**D**) Chemotaxis chambers were filled with medium by plugging ports 1 and 2 and then slowly injecting medium via port 3 until it emerged at port 4. Slow and steady filling can be achieved by turning the volume setting ring of a 20–100 µL volume pipette. After filling the first reservoir, the second reservoir can be filled by plugging ports 2 and 3 and then slowly injecting medium at port 4 until it emerges at port 1. (**E**) Phase-contrast image of the same observation area shown above (**C**) after filling the two reservoirs. Scale bar = 500 µm. Graphic elements provided by Elias Horn.

Figure 3: Chemotaxis assay. (**A**) Chemoattractant was introduced to one of the two reservoirs of a chemotaxis chamber by applying a 15 µL drop of medium containing 0.54 µg/mL complement C5a and 10 µg/mL Patent Blue V to filling port 1, followed by slow aspiration at port 4. (**B**) Initially after being drawn into the reservoir the blue, chemoattractant-containing medium had a roughly inverted drop shape, and then slowly diffused throughout the reservoir. (**C**) Migration tracks of macrophages migrating in a chemoattractant (complement C5a) gradient between 6–12 h after introducing chemoattractant to one of the reservoirs. The direction of the gradient is indicated on the right. The end of each migration track is indicated by a filled circle. (**D**) Blox plots of velocity, x-FMI (x-forward migration index) and y-FMI (y-forward migration index), an index of chemotactic efficiency that ranges from -1 to +1. Data were obtained by analysis of 25 macrophage migration tracks. Macrophages in the lower half of the observation area and showing displacement of at least one cell width over 6 h were randomly selected for analysis. Below is a plot of migration tracks after normalizing the start point to X = 0 and Y = 0. The chemotaxis index (y-FMI) was calculated by dividing the net displacement along the Y-axis (d) by

the accumulated length (l) of the migration path, as schematically shown. Graphic elements in panels A and B provided by Elias Horn.

Figure 4: Fluorescent images of living mouse resident peritoneal cells obtained by spinning disk confocal microscopy. (**A**) Extended focus image (brightest point merge of all Z-planes) of freshly isolated mouse peritoneal cells labeled with green fluorescent anti-F4/80 (macrophage marker) antibodies, red fluorescent anti-CD19 (B cell marker) antibodies, and a blue fluorescent nucleic acid stain. Scale bar = 10 µm. (**B**) Snapshot (single Z-plane) of $F4/80^+$ cells (macrophages) in the observation area of a chemotaxis chamber taken after an overnight chemotaxis assay. Cells were labeled with green fluorescent anti-F4/80 antibodies and a blue fluorescent nucleic acid stain. The complement C5a and Patent Blue V gradients were washed out by the cell labeling procedure, which explains why the upper reservoir in the schematic diagram of the chemotaxis chamber is not blue. Scale bar = 10 µm. Graphic element provided by Elias Horn.

DISCUSSION:

Intravital imaging dates back to the 19th century and provides a means to study the behavior of living immune cells in their natural environment. However, even with today's advanced microscopy and genetic techniques it is difficult to study the response of cells to specific chemoattractants in vivo. To circumvent this problem, Boyden[18] developed Transwell assays in the 1960s, but these end-point assays did not provide visualization of how cells actually migrated towards chemoattractants, making it difficult to distinguish chemokinesis, stimulated random migration by a chemical cue[32], and chemotaxis, migration towards higher concentrations of chemical stimuli from each other[33]. This problem was solved by designing various open chambers with a bridge, typically 1 mm wide, situated between two reservoirs and accessible by an objective lens[21-23]. Applying an inverted cover slip, seeded with adherent cells, closes the chambers and chemoattractant added to one of the reservoirs diffuses across the bridge to the opposing reservoir, creating a concentration gradient. Here we describe a chemotaxis assay using the same principle but using a closed chamber featuring four filling ports. Using this system and time-lapse, phase-contrast microscopy, we developed an assay to image mouse resident peritoneal macrophages migrating in a chemotactic complement C5a gradient[31,34-36]. This assay, combined with knockout mouse models, proved instrumental in the investigation of the roles of various Rho GTPases and motor proteins in macrophage morphology, motility, and chemotaxis[31,34-37]. We have also used this approach to image human peripheral blood monocytes migrating on a 2D surface or in a 3D collagen type I matrix[38]. Moreover, the assay is suitable for mouse bone marrow-derived macrophages or macrophages derived from conditionally immortalized myeloid precursor cells[39,40]. We have previously used polytetrafluoroethylene (PTFE) bags with luer adapters to culture bone marrow cells and obtain macrophages[34]. The advantage of PTFE bags is that the cells can be readily resuspended and ready for use after placing the bag on ice for 20–30 min. Note that we prefill the chemotaxis slide observation area before introducing the cells. This approach has the advantage that unwanted air bubbles can be subsequently flushed out (with variable success) and the presoaked observation area enables the slow introduction of a cell suspension by pipetting. Prefilling, though, increases the likelihood that the medium will partially flow into one or both of the flanking reservoirs, which will promote the seeding of cells beyond the observation area. Alternatively, the cell suspension can be directly

pipetted into a dry observation area, but unwanted air bubbles cannot be subsequently expelled.

The peritoneal cavity of the mouse contains two main populations of cells: F4/80$^+$ macrophages and (smaller) CD19$^+$ B cells, at a ratio of about 1:2 (**Figure 4A**). These two cell populations account for over 95% of peritoneal cavity cells, whereas the remaining F4/80$^-$/CD19$^-$ cells can usually be identified as CD11c$^+$ cells (dendritic cells) or CD3$^+$ cells (T cells). Weakly adherent B cells are washed out of the observation area during the filling of the reservoirs with the medium (**Figure 2**). After adding chemoattractant to one of the two reservoirs, time-lapse, phase-contrast microscopy can be used to image the remaining cells (macrophages) migrating in an evolving chemoattractant gradient. The formation of the complement C5a gradient in the observation area, via diffusion from one reservoir to the other, can be simulated using a fluorescent dye with similar molecular weight. A good substitute for recombinant mouse complement C5a (predicted molecular weight, 9.0 kDa) is fluorescently labeled dextran (10 kDa)[31]. Using confocal microscopy, the fluorescence gradient in the narrow channel (observation area) connecting the two reservoirs of the chemotaxis slide can be measured at fixed intervals and concentration profiles at the different time points can be plotted[24,31]. We routinely add a nonfluorescent, blue dye (Patent Blue V) to the chemoattractant medium to provide a convenient visual indicator of diffusion and gradient formation. Within 1 h of introducing 15 µL of blue, chemoattractant-containing medium into a reservoir, the reservoir appears uniformly blue and, according to Fick's laws of diffusion, a gradient will form across the narrow observation area connecting the reservoirs (**Figure 3B**). Several days are required for the solute (blue dye or chemoattractant) to become uniformly distributed.

Fluorescence microscopy can be substituted for phase-contrast microscopy, which offers advantages for automated cell tracking, because fluorescently labeled cells can be readily distinguished from the background. Another advantage is that specific populations of immune cells can be selectively tracked after labeling surface markers with fluorescent antibodies. We used this approach to image human peripheral blood CD14$^+$ cells (monocytes) migrating in a chemotactic fMLP (N-formylmethionine-leucyl-phenylalanine) gradient[38]. Similarly, fluorescent anti-F4/80 antibodies could be used to image mouse macrophages migrating in a chemotactic complement C5a gradient. Phototoxicity is a potential disadvantage of using fluorescence imaging[41]. This can be reduced by various means[42], including using fluorophores excited with longer wavelengths and adding antioxidants to the medium. Alternatively, labeled cells could initially be identified by fluorescence microscopy and subsequently imaged by time-lapse, phase-contrast microscopy. However, in practice, cells moving at moderately low velocities, such as ~1 µm/min (macrophages) or ~4 µm/min (monocytes), can be intermittently imaged by fluorescence microscopy at intervals of minutes, which is well tolerated[38]. We previously used fluorescence microscopy and the chemotaxis slide described here for 3D chemotaxis assays[38,43]. In this case, both reservoirs were prefilled with medium and 15 µL chemoattractant-containing medium was drawn into one of the reservoirs immediately before slowly pipetting fluorescently labeled cells suspended in medium containing collagen type I into the observation area. The difficult part of this procedure is the handling of collagen type I, which is concentrated in acidic solution. The pH of the collagen solution needs to be neutralized by addition of alkaline solution before mixing the ice-cold collagen solution with the cell suspension. Transfer of the collagen-

cell mixture to an incubator at 37 °C will initiate collagen polymerization. During incubation, the slide should be slowly rotated around its long axis so that the cells remain evenly distributed in the X-, Y- and Z-axis directions while the collagen polymerizes into a gel. A related closed chemotaxis slide suitable for 3D chemotaxis assays, with six plugs instead of four plugs, has recently been described[29]. This system allows the collagen-cell mixture to be introduced into the observation area before independently filling each of the flanking reservoirs, because each reservoir has two filling ports, rather than a single port.

In summary, we describe a real-time chemotaxis assay that allows the visualization of cells navigating in a chemotactic gradient over a period of 6 or more hours. Herein we focus on macrophages, which play major roles in inflammatory diseases but have been underrepresented in real-time chemotaxis assays compared to faster moving cells like neutrophils and *Dictyostelium* amoebae.

ACKNOWLEDGMENTS:

This work was supported by a grant (HA 3271/3-2) from the DFG (Deutsche Forschungsgemeinschaft).

DISCLOSURES:

The authors have nothing to disclose.

REFERENCES:

1. Lammermann, T., Germain, R. N. The multiple faces of leukocyte interstitial migration. *Seminars in Immunopathology*. **36**, 227–251 (2014).
2. Lammermann, T., Sixt, M. Mechanical modes of 'amoeboid' cell migration. *Current Opinion in Cell Biology.* **21**, 636–644 (2009).
3. Woodham, E. F., Machesky, L. M. Polarised cell migration: intrinsic and extrinsic drivers. *Current Opinion in Cell Biology.* **30**, 25–32 (2014).
4. Devreotes, P. N. et al. Excitable Signal Transduction Networks in Directed Cell Migration. *Annual Review of Cell and Developmental Biology.* **33**, 103–125 (2017).
5. Kamp, M. E., Liu, Y., Kortholt, A. Function and Regulation of Heterotrimeric G Proteins during Chemotaxis. *International Journal of Molecular Sciences.* **17** (1), 90 (2016).
6. Miao, Y. et al. Wave patterns organize cellular protrusions and control cortical dynamics. *Molecular Systems Biology.* **15**, e8585 (2019).
7. Ridley, A. J. et al. Cell migration: integrating signals from front to back. *Science.* **302**, 1704–1709 (2003).
8. Lammermann, T. et al. Rapid leukocyte migration by integrin-independent flowing and squeezing. *Nature.* **453**, 51–55 (2008).
9. Mullins, R. D., Heuser, J. A., Pollard, T. D. The interaction of Arp2/3 complex with actin: nucleation, high affinity pointed end capping, and formation of branching networks of filaments. *Proceedings of the National Academy of Sciences of the United States of America.* **95**, 6181–6186 (1998).
10. Leithner, A. et al. Diversified actin protrusions promote environmental exploration but are dispensable for locomotion of leukocytes. *Nature Cell Biology.* **18**, 1253–1259 (2016).

11. McDonald, B. et al. Intravascular danger signals guide neutrophils to sites of sterile inflammation. *Science.* **330**, 362–366 (2010).
12. Leber, T. Ueber die Entstehung der Entzündung und die Wirkung der entzündungserregenden Schädlichkeiten. *Fortschritte der Medizin.* **6**, 460–464 (1888).
13. Tauber, A. I. Metchnikoff and the phagocytosis theory. *Nature Reviews Molecular Cell Biology.* **4**, 897–901 (2003).
14. Clark, E. R., Linton Clark, E. Reactions of cells in the tail of amphibian larvae to injected croton oil (aseptic inflammation). *American Journal of Anatomy.* **27**, 221–254 (1920).
15. Clark, E. R., Linton Clark, E. The reaction of living cells in the tadpole's tail toward starch, agar-agar, gelatin, and gum arabic. *The Anatomical Record.* **24** (1922).
16. Comandon, J. Phagocytose in vitro des Hématozoaires du Calfat (enregistrement cinématographique). *Comptes Rendus Hebdomadaires des Séances et Mémoires de la Société de Biologie.* **69**, 314–316 (1917).
17. McCutcheon, M. Chemotaxis in leukocytes. *Physiological Reviews.* **26**, 319–336 (1946).
18. Boyden, S. The chemotactic effect of mixtures of antibody and antigen on polymorphonuclear leucocytes. *The Journal of Experimental Medicine.* **115**, 453–466 (1962).
19. Horwitz, D. A., Garrett, M. A. Use of leukocyte chemotaxis in vitro to assay mediators generated by immune reactions. I. Quantitation of mononuclear and polymorphonuclear leukocyte chemotaxis with polycarbonate (nuclepore) filters. *Journal of Immunology.* **106**, 649–655 (1971).
20. Bignold, L. P. A novel polycarbonate (Nuclepore) membrane demonstrates chemotaxis, unaffected by chemokinesis, of polymorphonuclear leukocytes in the Boyden chamber. *Journal of Immunological Methods.* **105**, 275–280 (1987).
21. Zigmond, S. H. Ability of polymorphonuclear leukocytes to orient in gradients of chemotactic factors. *The Journal of Cell Biology.* **75**, 606–616 (1977).
22. Zicha, D., Dunn, G. A., Brown, A. F. A new direct-viewing chemotaxis chamber. *Journal of Cell Science.* **99** (Pt 4), 769–775 (1991).
23. Muinonen-Martin, A. J., Veltman, D. M., Kalna, G., Insall, R. H. An improved chamber for direct visualisation of chemotaxis. *PLoS One.* **5**, e15309 (2010).
24. Zengel, P. et al. mu-Slide Chemotaxis: a new chamber for long-term chemotaxis studies. *BMC Cell Biology.* **12**, 21 (2011).
25. Valentim, A. M., Guedes, S. R., Pereira, A. M., Antunes, L. M. Euthanasia using gaseous agents in laboratory rodents. *Lab Animal*. **50**, 241–253 (2016).
26. Franks, N. P. General anaesthesia: from molecular targets to neuronal pathways of sleep and arousal. *Nature Reviews. Neuroscience.* **9**, 370–386 (2008).
27. Cordelieres, F. P. et al. Automated cell tracking and analysis in phase-contrast videos (iTrack4U): development of Java software based on combined mean-shift processes. *PLoS One.* **8**, e81266 (2013).
28. Zantl, R., Horn, E. Chemotaxis of slow migrating mammalian cells analysed by video microscopy. *Methods in Molecular Biology.* **769**, 191–203 (2011).
29. Biswenger, V. et al. Characterization of EGF-guided MDA-MB-231 cell chemotaxis in vitro using a physiological and highly sensitive assay system. *PLoS One.* **13**, e0203040 (2018).
30. Austyn, J. M., Gordon, S. F4/80, a monoclonal antibody directed specifically against the mouse macrophage. *European Journal of Immunology.* **11**, 805–815 (1981).

31. Hanley, P. J. et al. Motorized RhoGAP myosin IXb (Myo9b) controls cell shape and motility. *Proceedings of the National Academy of Sciences of the United States of America.* **107**, 12145–12150 (2010).
32. Wilkinson, P. C. Cell Locomotion and Chemotaxis: Basic Concepts and Methodological Approaches. *Methods.* **10**, 74–81 (1996).
33. Pfeffer, W. Locomotorische Richtungsbewegungen durch chemische Reize. *Untersuchungen aus dem Botanischen Institut zu Tübingen.* **1**, 363–482 (1884).
34. Konigs, V. et al. Mouse macrophages completely lacking Rho subfamily GTPases (RhoA, RhoB, and RhoC) have severe lamellipodial retraction defects, but robust chemotactic navigation and altered motility. *The Journal of Biological Chemistry.* **289**, 30772–30784 (2014).
35. Horsthemke, M. et al. Multiple roles of filopodial dynamics in particle capture and phagocytosis and phenotypes of Cdc42 and Myo10 deletion. *The Journal of Biological Chemistry.* **292**, 7258–7273 (2017).
36. Bachg, A. C. et al. Phenotypic analysis of Myo10 knockout (Myo10(tm2/tm2)) mice lacking full-length (motorized) but not brain-specific headless myosin X. *Scientific Reports.* **9**, 597 (2019).
37. Horsthemke, M. et al. A novel isoform of myosin 18A (Myo18Agamma) is an essential sarcomeric protein in mouse heart. *The Journal of Biological Chemistry.* **294**, 7202–7218 (2019).
38. Bzymek, R. et al. Real-time two- and three-dimensional imaging of monocyte motility and navigation on planar surfaces and in collagen matrices: roles of Rho. *Scientific Reports.* **6**, 25016 (2016).
39. Wang, G. G. et al. Quantitative production of macrophages or neutrophils ex vivo using conditional Hoxb8. *Nature Methods.* **3**, 287–293 (2006).
40. Gran, S. et al. Imaging, myeloid precursor immortalization, and genome editing for defining mechanisms of leukocyte recruitment in vivo. *Theranostics.* **8**, 2407–2423 (2018).
41. Magidson, V., Khodjakov, A. Circumventing photodamage in live-cell microscopy. *Methods in Cell Biology.* **114**, 545–560 (2013).
42. Icha, J., Weber, M., Waters, J. C., Norden, C. Phototoxicity in live fluorescence microscopy, and how to avoid it. *BioEssays : News and Reviews in Molecular, Cellular and Developmental Biology.* **39** (8), 1700003 (2017).
43. Isfort, K. et al. Real-time imaging reveals that P2Y2 and P2Y12 receptor agonists are not chemoattractants and macrophage chemotaxis to complement C5a is phosphatidylinositol 3-kinase (PI3K)- and p38 mitogen-activated protein kinase (MAPK)-independent. *The Journal of Biological Chemistry.* **286**, 44776–44787 (2011).

Figure 1

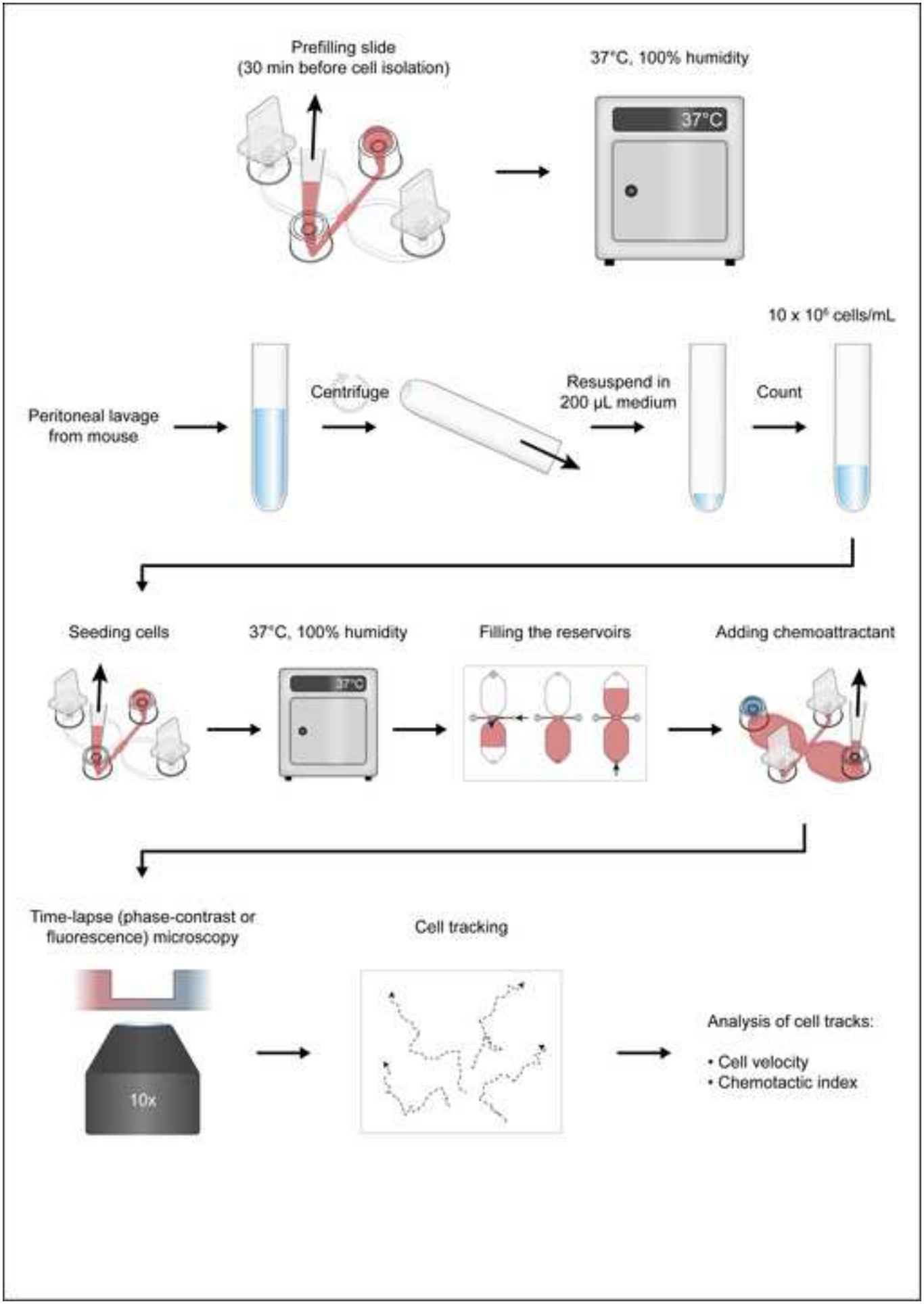

Figure 2

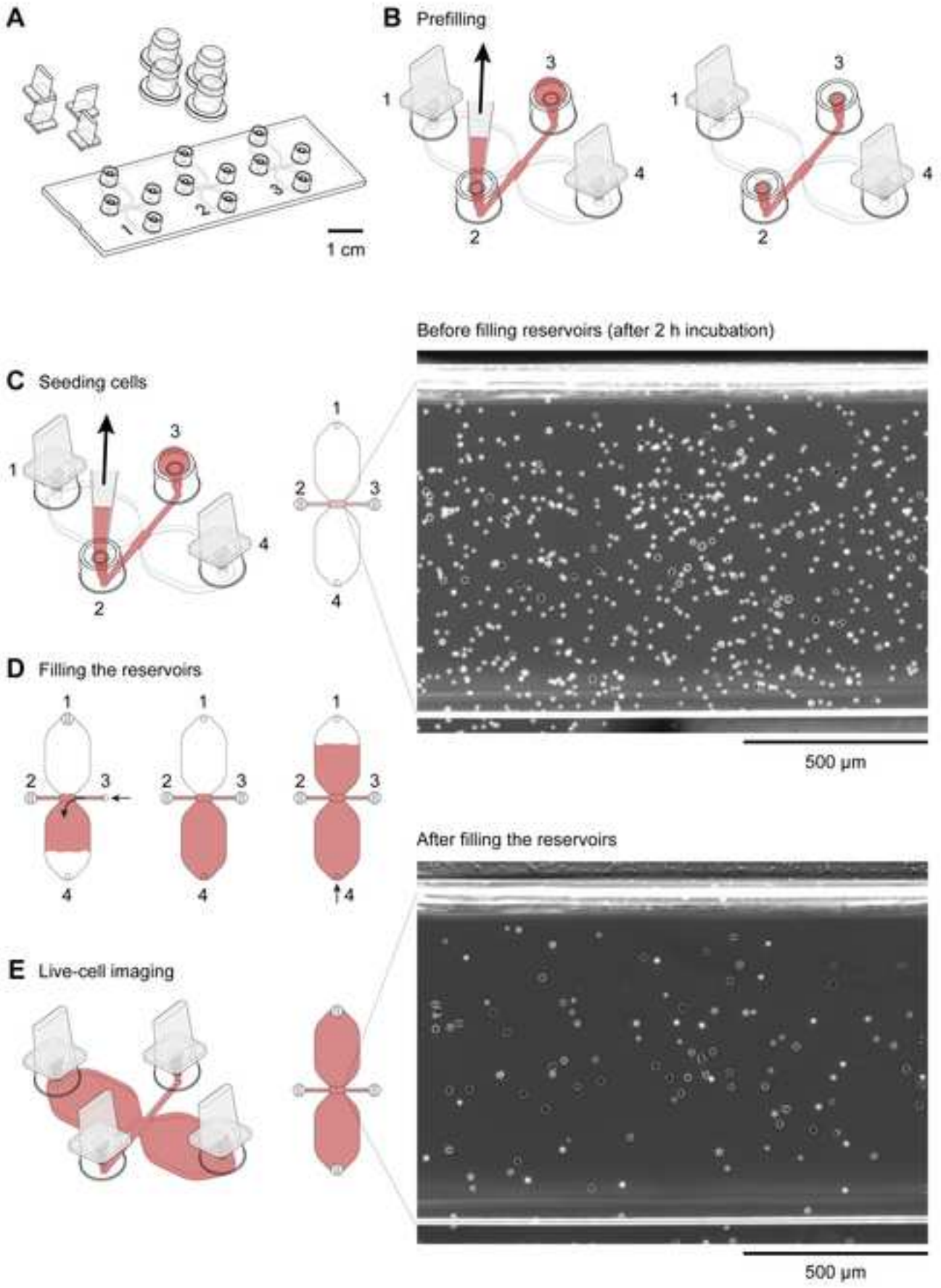

Figure 3

Click here to access/download;Figure;Figure 3.tif

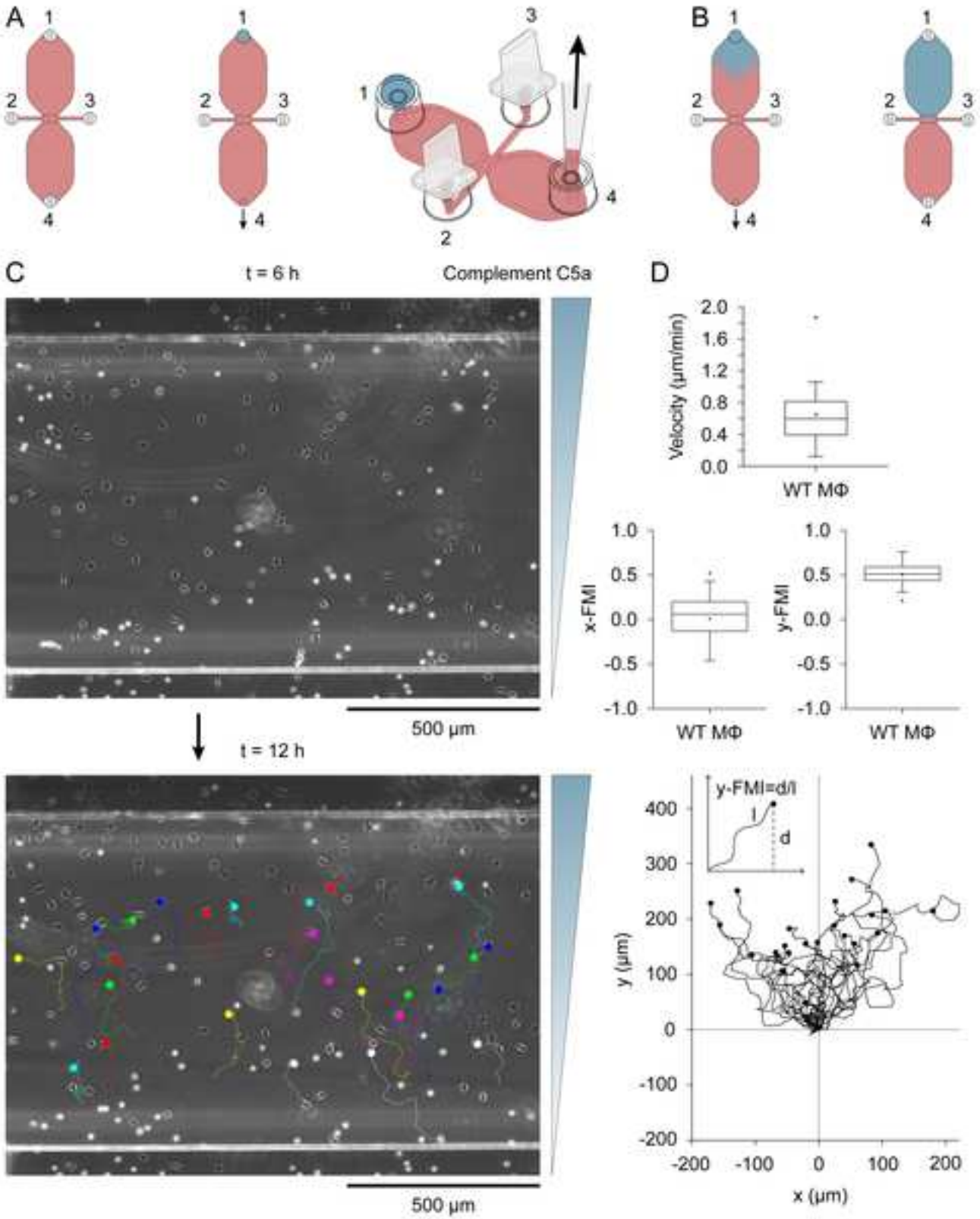

Figure 4

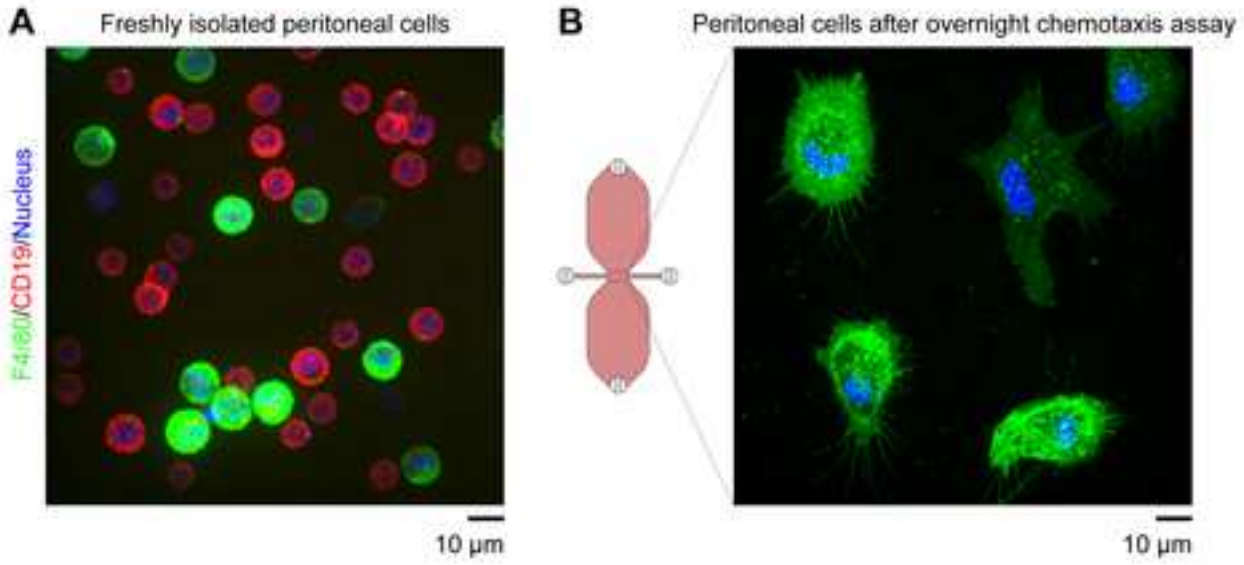

Name of Material/ Equipment	Company
µ-Slide (anodized aluminium) rack	Ibidi, Martinsried, Germany
µ-Slide Chemotaxis 2D (chemotaxis slide)	Ibidi, Martinsried, Germany
100x penicillin/streptomycin	Thermo Fisher Scientific
10-100 µL pipette with volume control ring	Eppendorf
10-200 µL pipette tips	Greiner Bio-One International
14 ml polypropylene round bottom tubes	BD Falcon
14-bit Hamamatsu C9100-50 Electron Multiplying-Charged Couple Device (EM-CCD) peltier-cooled camera	Hamamatsu Photonics Inc., Japan
2-20 µL pipette with volume control ring	Eppendorf
24-G plastic catheter	B Braun Mesungen AG, Germany
405 nm solid state laser, 50 mW	Perkin Elmer, Rodgau, Germany
488 nm solid state laser, 50 mW	Perkin Elmer, Rodgau, Germany
561 nm solid state laser, 50 mW	Perkin Elmer, Rodgau, Germany
Alexa Fluor 488-conjugated rat (IgG2a) monoclonal (clone BM8) anti-mouse F4/80 antibody	Thermo Fisher Scientific
Alexa Fluor 594-conjugated rat (IgG2a) monoclonal (clone 6D5) anti-mouse CD19 antibody	BioLegend
C-Chip disposable (improved Neubauer) hemocytometer	NanoEnTek (distributed by VWR International)
CSU-X1 spinning disk scanner	Yokogawa Electric Corporation, Japan
Hank's buffered salt solution without Ca^{2+} and Mg^{2+}	Thermo Fisher Scientific
Heat-inactivated fetal bovine serum	Thermo Fisher Scientific
Hoechst 34580	Thermo Fisher Scientific
ImageJ (image processing and analysis in Java)	National Institutes of Health (NIH)
Lipopolysaccharides from *Escherichia coli* O111:B4	Sigma-Aldrich
Nikon Eclipse Ti inverse microscope	Nikon, Japan
Patent Blue V, sodium salt	Sigma-Aldrich
Recombinant mouse complement C5a protein	R&D Systems
RPMI 1640 medium containing 20 mM Hepes	Sigma-Aldrich
UltraVIEW Vox 3D live cell imaging system + Volocity software	Perkin Elmer, Rodgau, Germany
Zeiss LSM 510 + Axiovision software	Carl Zeiss Microscopy, Oberkochen, Germany

Catalog Number	Comments/Description
80003	Autoclavable stackable rack for channel slides
80306	Slide containing chemotaxis chambers (tissue culture treated)
15140122	Used as supplement for RPMI 1640 media
3123000047	Eppendorf Research plus pipette
739261	Pipette tips with beveled tips (96 pieces per rack: sterile)
352059	Used to collect peritoneal cells
	EM-CCD camera of the spinning disk confocal microscope system
3123000039	Eppendorf Research plus pipette
4254503-01	Used for peritoneal lavage
	Laser (405 nm) source of spinning disk confocal microscope system
	Laser (488 nm) source of spinning disk confocal microscope system
	Laser (561 nm) source of spinning disk confocal microscope system
MF48020	Mouse macrophage marker and plasma membrane label
115552	Mouse B cell marker
631-1098	Used to count cells
	Nipkow spinning disk unit
14170120	Used for peritoneal lavage
10082139	Used as supplement for RPMI 1640 media
H21486	Cell permeable, blue fluorescent nucleic acid stain
	Image analysis software
L4391-1MG	Toll-like receptor 4 ligand
	Inverted microscope
21605-10G	Blue-colored dye used as visual indicator of gradient formation
2150-C5-025	Chemoattractant for mouse macrophages
R7388	Basis medium for assays
	Spinning disk confocal microscope system
	Confocal laser scanning microscope (LSM) adapted for phase-contrast microscopy

JoVE submission JoVE60750
Manuscript title: Time-lapse imaging of mouse macrophage chemotaxis

Response to Editorial comments

Thank you for the guidelines and suggestions.

1. Done
2. Text revised
3. Key words added
4. Protocol modified
5. Excess text removed
6. Surgical tool(s) specified
7. Text for video: highlighted yellow
8. Complete sentences highlighted
9. Figures provided as .tiff
10. Materials are now sorted alphabetically by the material name

Response to Revierwer #1

Thank you for reading the manuscript and for your many helpful suggestions.

Minor concerns:
(Lines refer to originally submitted manuscript)

Lines 46-50: Changes made, except we deleted "particularly . . ." in response to related comments from with Reviewer #2.

Lines 56-57: Neutrophils and *D. discoideum* are commonly used models of chemotaxis and the assays are typically performed using a point-source of chemoattractant. However, this approach is unsuitable for slow moving macrophages. Much of our knowledge and theories of chemotaxis have come from experiments using *D. discoideum* and, thus, we would prefer to mention both models in this sentence.

Line 62: The relative clause has now been deleted.

Line 66: Done.

Introduction: The second paragraph of the Introduction now describes various chemoattractants, including the chemokine family and its classification into structurally related peptides.

Lines 88-89: I have changed the text and added a linking sentence.

Lines 99-100: The sentence has been modified.

Note that transwell or transendothelial migration assays do not provide a possibility to monitor cell navigation in a chemotactic gradient since the cells only move across a structure no more than one cell diameter thick.

We do not seek to strictly emulate *in vivo* conditions with this particular mouse macrophage 2D chemotaxis assay, although the notion is attractive. The next obvious step would be to perform 3D chemotaxis assays using a physiological matrix, such as collagen type I matrices, or perhaps after seeding the chemotaxis chamber with mesothelial cells to simulate the lining of the peritoneal cavity. We used, for example, 3D collagen matrices in the past to study the chemotaxis of human monocytes using time-lapse fluorescence microscopy, which worked very well. We also tested mesentery (parietal peritoneal) patches, isolated with the help of 6 mm (inner diameter) ring magnets, as potential *ex vivo* structures to study macrophage motility in a natural environment, but these preparations proved unsuitable, at least in our hands. In the end, our current mouse macrophage 2D chemotaxis assay has proven to be the most helpful approach to study macrophage motility and chemotaxis. In fact, it

is difficult to find an equivalent assay for macrophages in the literature. A great deal of knowledge on cell motility and chemotaxis has been gained using 2D chemotaxis assays, for example, the large body of work from Peter N. Devreotes and many others is derived from 2D motility assays.

Line 130: The reference to Figure 1A has been moved to another sentence in Section 1.1.

Line 177: The sentence containing Neubauer has been modified to include other counting devices.

Lines 178-180: The following sentence has been added: "The round-bottom tube allows the supernatant to be fully decanted and reduces cell clumping."

Line 261: Done.

Lines 288-290: Fluorescence labeling of cells for flow cytometry or immunofluorescence imaging is a standard procedure. A description of the labeling would create a digression from the main protocol, a chemotaxis assay using time-lapse, phase-contrast microscopy. The cell labeling and fluorescence imaging serves to underscore that two major populations of cells ($F4/80^+$ cells and $CD19^+$ cells) are obtained following peritoneal lavage. This point should be stressed in the protocol, which is specific for mouse resident peritoneal macrophages.

Lines 290-291: It is important to stress that F4/80 is a specific marker for mouse macrophages and mouse peritoneal B cells are $CD19^+$. That is, the cells are not identified by relative intensities, such as $F4/80^{hi}/CD19^{lo}$ or $CD19^{hi}/F4/80^{lo}$ etc.

Lines 298-299: This is a good point. Patent Blue V has a molecular weight of about 0.6 kDa, whereas recombinant mouse complement C5a is about 9 kDa. Thus, Patent Blue V has a higher diffusion coefficient than complement C5a. Nevertheless, using Patent Blue V it is possible to visualize how the chemoattractant-containing medium is drawn into the reservoir and how it diffuses until the reservoir is uniformly blue. In the following 1-2 days it is hard to detect the blue dye in the other (opposing) reservoir by visual inspection. This underscores the effectiveness of the system. That is, one can "see" that a gradient has been generated across the narrow connecting area. Even better, the chemoattractant lags behind the smaller blue dye, so that the complement C5a gradient is even longer lasting. Notably, it is good that the gradient is dynamic, steadily growing, because this is how gradients occur *in vivo*, that is, gradients are not static, but dynamic. In the past, to take into account molecular weight differences, we have measured, or approximated, the kinetics of the complement C5a gradient using a fluorescent dye with similar weight to complement C5a, such as 10 kDa fluorescent dextran.

Line 304: Thanks for spotting this. The reference has been added.

Lines 355-356: The following sentence was added: "Macrophages in the lower half of the observation area and showing displacement (movement) of at least one cell width over 6 h were randomly selected for analysis."

Lines 369-370: Chemicals, such as lipopolysaccharides or other Toll-like receptor ligands, may stimulate motility (chemokinesis) without having chemotactic activity.

Line 389: Thioglycolate would induce sterile inflammation (peritonitis) which would attract various immune cells, including neutrophils, followed by monocytes. After 1-2 days, the peritoneal cavity will potentially contain a heterogenous population of cells, including resident peritoneal macrophages, monocyte-derived macrophages and neutrophils, although an enriched population of macrophages can be obtained in the appropriate time window etc. The intraperitoneal injection of thioglycolate also introduces ethical considerations since a proinflammatory procedure is performed on a living animal. Moreover, more resident peritoneal macrophages are obtained than are required for filling 6, 12 or even more chemotaxis slides, each of which only requires 10 µL of cell suspension with a concentration of 10×10^6 cells/mL. The weakly adherent B cells are generally washed away during the filling procedure.

Line 435: That is correct, although we had written in the next sentence: “However, the time-lapse 2D chemotaxis assay described herein can be adapted to a 3D chemotaxis assay and both assays are suitable for phase-contrast and/or fluorescence microscopy and can be adapted for different cell types.”
The summary (last paragraph of the Discussion), which included the above text, was rewritten in response to suggestios from Reviewer #2. The summary now reads:
“In summary, we describe a real-time chemotaxis assay which allows the visualization of cells navigating in a chemotactic gradient over a period of six or more hours. Herein the assay has been customized for macrophages, which play major roles in inflammatory diseases, but have traditionally been circumvented in favor of faster moving cells like neutrophils and *Dictyostelium* amoebae.”

Response to Reviewer #2

Thank you for your detailed input and suggestions to improve the manuscript.

(Lines refer to originally submitted manuscript)

1. Line 46: Now deleted.
2. Line 52-53: Good point. We have interposed a new paragraph which elaborates on chemokines (as suggested by Reviewer #1) and makes a link to the next paragraph.
3. Abstract: We have extended the last sentence of the Abstract to highlight the advantage of the system. We have, for example, used this system together with knockout mouse models to identify the roles of G protein subunits in chemotaxis (manuscript complete).
4. Line 72: The reference was added to Line 73 of the originally submitted manuscript.
5. Start of Protocol Section: Good idea. A workflow diagram is now included.
6. Line 157: Reviewer #1 made a similar suggestion. The reply to Reviewer #1 is pasted below.
“Thioglycolate would induce sterile inflammation (peritonitis) which would attract various immune cells, including neutrophils, followed by monocytes. After 1-2 days, the peritoneal cavity will potentially contain a heterogenous population of cells, including resident peritoneal macrophages, monocyte-derived macrophages and neutrophils, although an enriched population of macrophages can be obtained at the appropriate time window etc. The intraperitoneal injection of thioglycolate introduces ethical considerations since a proinflammatory procedure is performed on a living animal. Moreover, more resident peritoneal macrophages are obtained than are required for filling 6, 12 or even more chemotaxis slides, each of which only requires 10 µL of cell suspension with a concentration of 10×10^6 cells/mL. The weakly adherent B cells are generally washed away during the filling procedure.”
7. Lines 165-166: Good point. We presume that *in vivo* resident peritoneal macrophages weakly adhere to the mesothelium lining the peritoneal cavity and/or are simply in suspension in an inactivated state. Nominally Ca^{2+}-free HBSS was used since the low [Ca^{2+}] may reduce integrin-dependent adhesion. As far as we are aware, Ca^{2+}-free, bicarbonate-free RPMI 1640 Hepes medium is not a standard, readily available formulation.
8. Line 173: For economy, in accord with the Editorial comments, we deleted some text, part of which included reference to abdominal massage. In any case, we gently massage the abdomen for about 10 s.
9. Lines 177-178: The typical number of cells obtained per mouse has been added.
10. Lines 183-184: Positive or negative selection methods would introduce more interventions. We prefer to minimize the handling of the cells.
In the originally submitted manuscript, we wrote in the Discussion:
“Fluorescence microscopy can be substituted for phase-contrast microscopy, which offers advantages for automated cell tracking, since fluorescently labeled cells can be

readily distinguished from the background. Another advantage is that specific populations of immune cells can be selectively tracked after labeling surface markers with fluorescent antibodies. We used this approach for imaging human peripheral blood $CD14^+$ cells (monocytes) migrating in a chemotactic FMLP (N-formylmethionine-leucyl-phenylalanine) gradient[36]."

We now added the sentence:

"Similarly, fluorescent anti-F4/80 antibodies could be used to image mouse macrophages migrating in a chemotactic complement C5a gradient."

11. Line 188: The mixing procedure has been elaborated:
"After pipetting the cell suspension up and down five times with the pipette volume set at 100 µL (or set at half the suspension volume) to reduce clumping … ".
12. Good point. The order of figures was based on the Results section. We have now based the order on the main text (Protocol + Results) and accordingly changed the order of the figures.
13. Lines 225-228: The paragraph has been rephrased.
14. Line 244: The figure reference has been added (Fig. 2 has become Fig. 3 in the revised manuscript).
15. Line 247: See response number 10 above. Indeed, fluorescence labeling would be more reliable than morphological criteria.
16. Line 256: The analysis section has been modified. The link between iTrack4U and ImageJ was misleading and the text has been reworded accordingly. Both programs are Java-based, but iTrack4U is a stand alone program for automated tracking and analysis. The first author of the paper describing iTrack4U (Fabrice P. Cordelières) also produced the ImageJ plugin Manual Tracking. The manual tracking datasets can be automatically analyzed by the ImageJ plugin Chemotaxis and Migration Tool. This is now clearly stated with references.
17. Figures 3D and 3E are now combined into Figure 3D. It would have been more logical to present the migration plot above the box plots of velocity and FMIs, but we wanted to have the original tracks and the migration plot side-by-side, as it is in the figure.
18. Line 307: See response number 17 above.
19. Line 354-359: We have included a box plot of x-FMI values.
20. Line 385-387 and Figure 3D: We suggested an alternative method in the originally submitted manuscript, i.e. by skipping the prefilling step the risk that medium flows into a reservoir is reduced:
"Prefilling, though, increases the likelihood that medium will partially flow into one or both of the flanking reservoirs, which will promote the seeding of cells beyond the observation area. Alternatively, the cell suspension can be directly pipetted into a dry observation area, but unwanted air bubbles cannot be subsequently expelled."
The flow of a small amount of cell suspension into the reservoirs during cell seeding is not solely disadvantageous since the pool of cells can be recruited into the observation area.
21. Line 436-449: The summary has been modified.
22. Discussion: We added the sentences: "Moreover, the assay is suitable for mouse bone marrow-derived macrophages or macrophages derived from conditionally immortalized myeloid precursor cells[39,40] We have previously used Teflon bags with luer adapters to culture bone marrow cells and derive macrophages[34]. The advantage of Teflon bags is that the cells can be readily resuspended, ready for use, after placing a bag on ice for 20-30 min."
23. Materials: The software used for acquiring images and the image analysis software are now provided in the tabulated Materials section.
24. Figure 3D: Fig. 3D is now Fig. 2D. The x-axes are now labeled.

25. Figure 3A: Good point. The “end” of each migration track was indicated by a filled circle, albeit it was too small to readily recognize. We have now enlarged the filled spots so that the end of each track is now clear. This is now indicated in the legend.
26. Figure 3A: An approximate scale bar has been incorporated.
27. Materials: The tabulated Materials section is an Excel (.xls) file with four columns: Name of Material/Equipment, Company, Catalog number and Comments/Description. Catalog numbers have been provided where appropriate.